Supplementary Figure 1. CLIC1 expression level in human glioblastomas. (A and B) Association of CLIC1 mRNA levels with GBM subtypes (Proneural [PN], Proliferative [Prolif], Neural [N], Classical [CL] and Mesenchymal [MES]). Data from LBL 202 (A) and UNC 202 (B) microarrays derived from Verhaak's work were examined. In each graph, the solid lines within the boxes represent the median value; the boxes show the 25th and 75th percentile range of CLIC1 mRNA levels; maximum and minimum values are depicted as horizontal bars; circles represent outliers. *** p-value < 0.0001 between indicated pairs calculated by ANOVA with Tamhane's multiple comparison test; n.s.: not significant.

Supplementary Figure 1

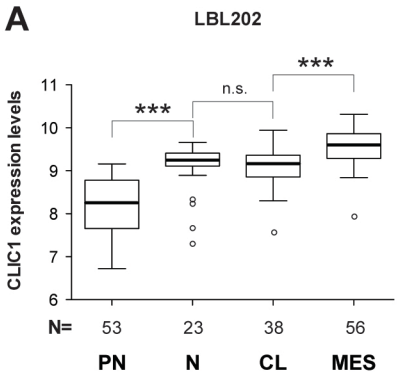

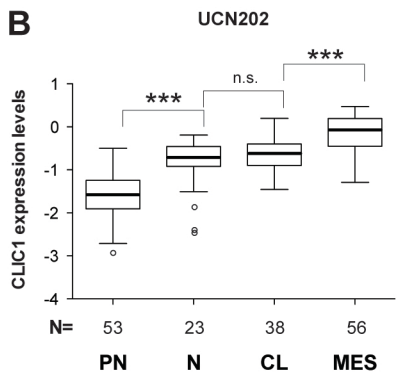

Supplementary Figure 2. Immunofluorescent staining to validate the specificity of CLIC1 antibody. Signal specificity is demonstrated by CLIC1 immunofluorescent staining of mouse embryonic fibroblasts derived from wild-type (MEF wt) and CLIC1 knocked out mice (MEF CLIC1-KO) (CLIC1, red; DAPI: blue). Scale bar = 50 μm.

Supplementary Figure 2

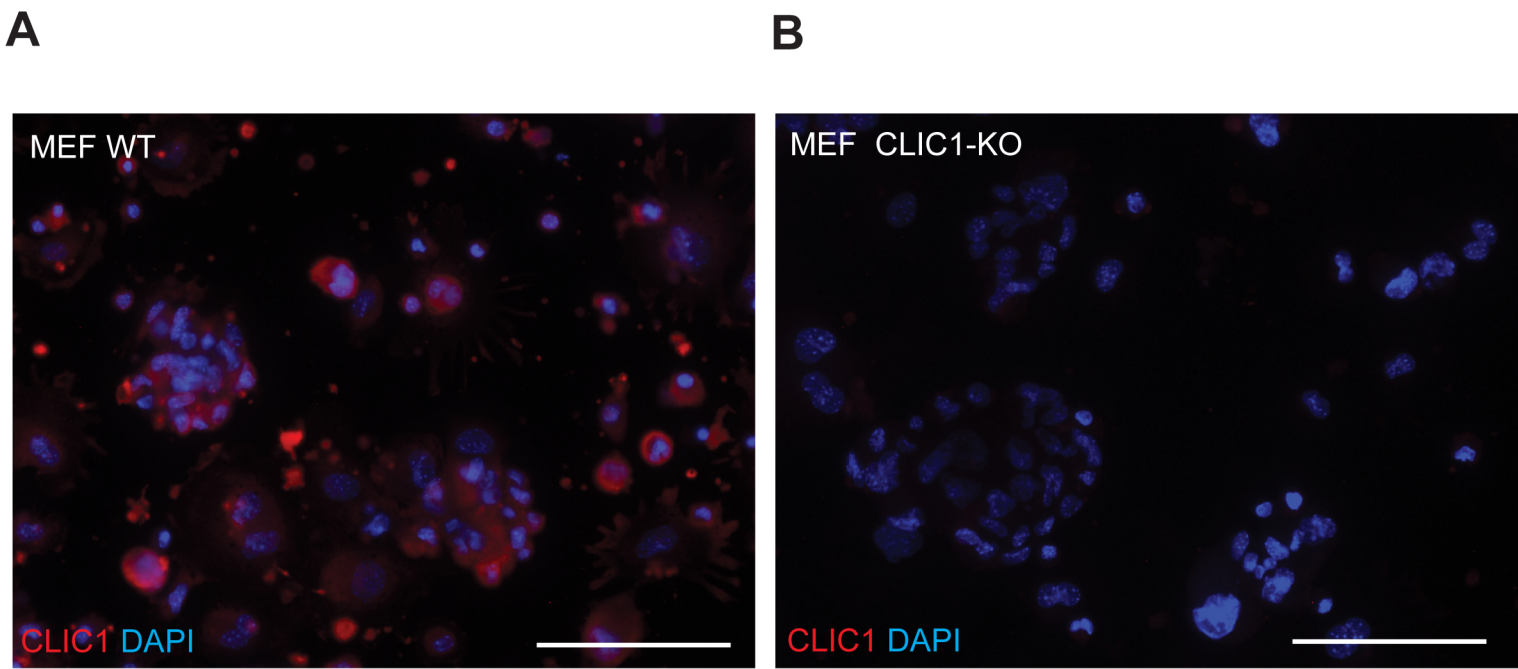

Supplementary Figure 3. CLIC1 subcellular localization in normal and tumoral neurospheres. (A and B) Representative images of CLIC1 immunostaining in not permeabilized human GBM neurospheres (A) and normal (mNSCs) and tumoral mouse neurospheres (GL261) (B). Dissociated neurospheres were fixed and processed for immunofluorescence (CLIC1, red; DAPI: blue). Cells were analyzed using confocal laser scanning microscopy and a single optical x-y-plane section is shown. Scale bar = 10 µm. hGBM#8, hGBM#10 and hGBM#23: neurospheres isolated from three GBM patients; mNSCs: murine neural stem cells; GL261: murine GBM neurospheres; (C) Western blotting analysis of CLIC1 expression levels in plasma-membrane and cytoplasm-containing fractions derived from normal (mNSC) and tumoral mouse neurospheres (GL261). Na^+,K^+ Pump and GAPDH expression were examined to assess the purity of plasma-membrane and cytoplasmic fractions respectively. Reversible Ponceau staining was used as a control for equal protein loading. (D) CLIC1-mediated Cl^- currents measured by perforated patch clamp technique in normal (mNSC) and tumoral (GL261) neurospheres. Cl^- currents mediated by CLIC1 (I_{IAA94}) were isolated using the specific CLIC1 inhibitor indanyloxyacetic acid–94 (IAA94), and normalized to the total cell current (I_{Tot}) (I_{IAA94}/I_{Tot}%). Average values derived from five independent experiments were represented. Error bars represent 95% confidence intervals. $p<0.001$. GLM test of between-subjects effects: F for "potential" = 0.103, d. f. = 5, p = 0.991 (n. s.); F for "cell type" = 13.442, d. f. = 1, p = 0.001; F for variables interaction = 0.294, d. f. = 5, p = 0.914 n. s. No significance for interaction means a similar pattern of I_{IAA94} / I_{Tot} change for different cell types at different membrane potential values, even if average I_{IAA94} / I_{Tot} values are different between different cell types.

Supplementary Figure 3

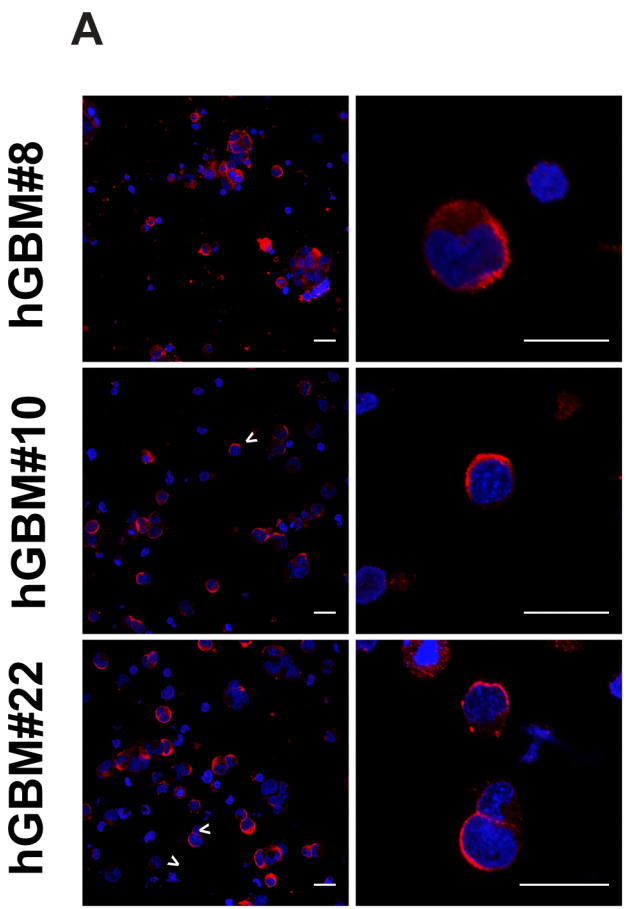

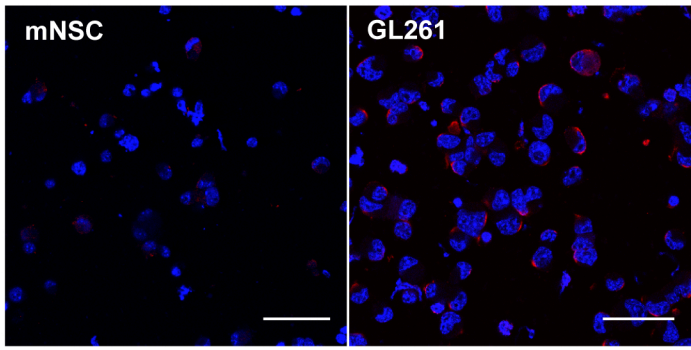

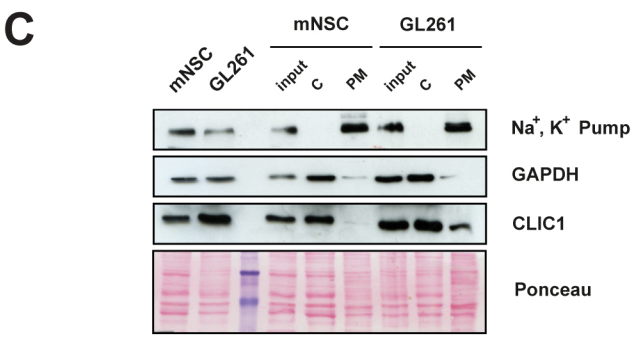

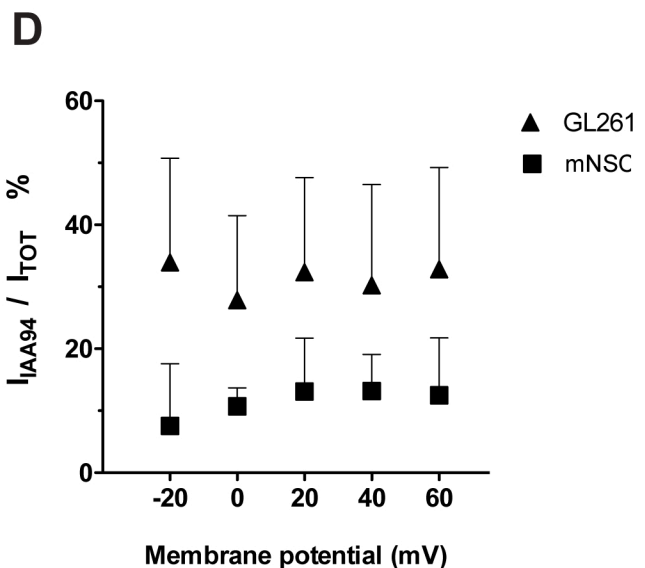

Supplementary Figure 4. Effect of CLIC1 silencing in GBM neurospheres. (A) Western blotting analysis showing the efficiency of CLIC1 silencing in GBM neurospheres isolated from two patient samples. Dissociated neurospheres were transduced with lentivirus carrying either non-targeting shRNA (NT) or CLIC1 shRNA (sh). Vinculin was used as loading control. (B and D) Representative current traces (total, IAA94 sensitive and DIDS sensitive currents) recorded in the perforated patch configuration from NT (B) and CLIC1 silenced (sh) (D) cells derived from hGBM#7 cells, and elicited by different potential steps (from -60 mV to 60 mV). (C and E) The current-voltage relationships for the corresponding experiments in (B and D). (F) CLIC1 sensitive currents (I_{IAA94}) were isolated using the specific CLIC1 inhibitor indanyloxyacetic acid–94 (IAA94), and normalized to the total cell current (I_{Tot}) (I_{IAA94}/I_{Tot}%). (G) The other Cl^- currents in the cells were evaluated by the inhibitor 4,4'-Diisothiocyano-2,2'-stilbenedisulfonic acid (I_{DIDS}) and normalized to the total cell current (I_{Tot}) (I_{DIDS}/I_{Tot}%). For results in panels (F and G), average values derived from four independent experiments were represented. Error bars represent 95% confidence intervals. GLM test of between-subjects effects on I_{IAA94} / I_{Tot} values: F for "potential" = 0.167, d. f. = 4, p = 0.953 (n. s.); F for "cell type" = 84.804, d. f. = 1, $p < 0.001$; F for variables interaction = 0.533, d. f. = 4, p = 0.713 n. s. No significance for interaction means a similar pattern of I_{IAA94}/I_{Tot} change for different cell types at different membrane potential values, even if average I_{IAA94}/I_{Tot} values are different between different cell types. GLM test of between-subjects effects on I_{DIDS}/I_{Tot} values: F for "potential" = 2.086, d. f. = 4, p = 0.113; F for "cell type" = 0.900, d. f. = 1, p = 0.352; F for variables interaction = 0.069, d. f. = 4, p = 0.991. No significance for interaction means a similar pattern of I_{DIDS}/I_{Tot} change for different cell types at different membrane potential values.

Supplementary Figure 4

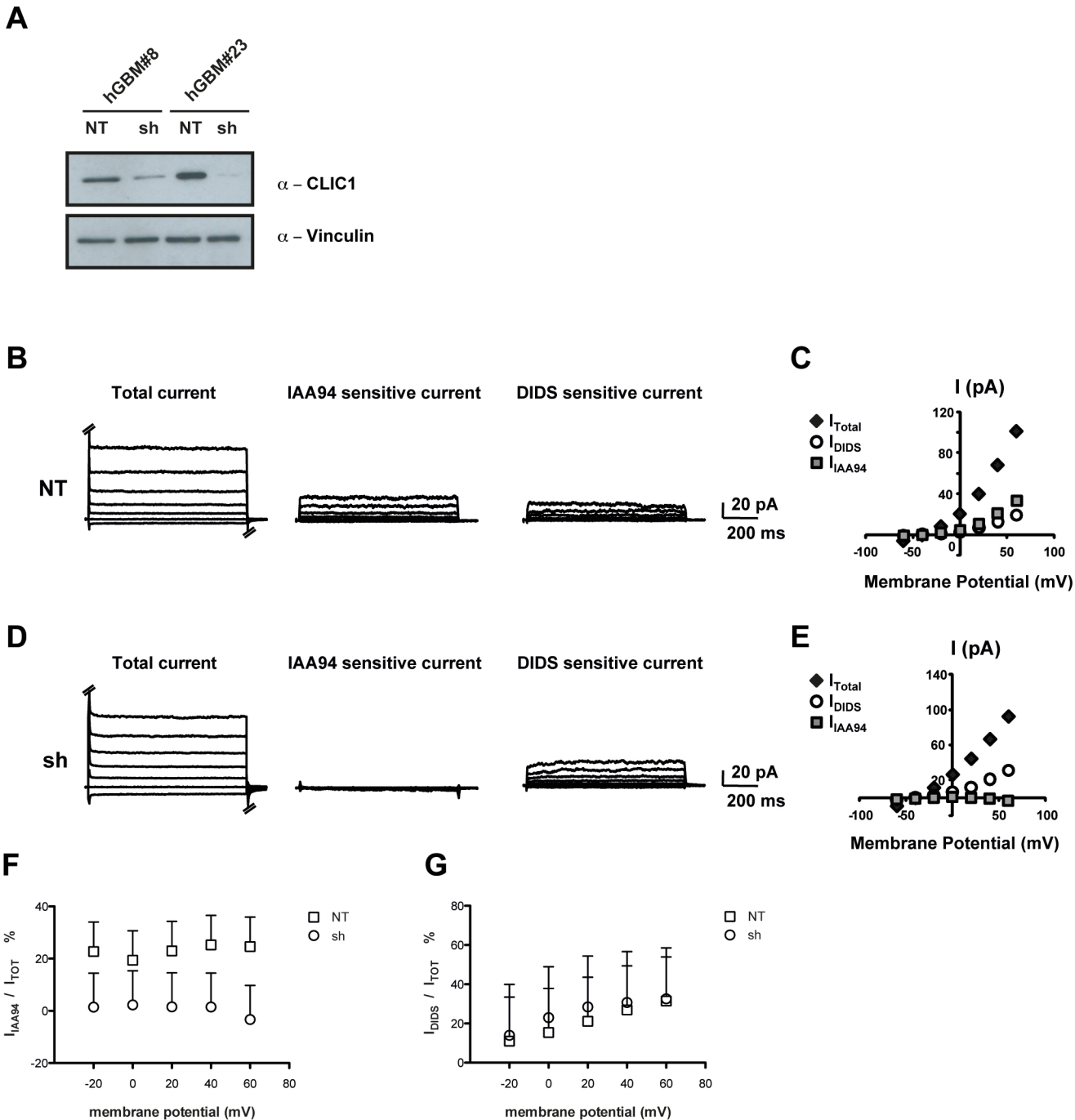

Supplementary Figure 5. Effects of CLIC1 silencing on clonogenicity and proliferation of GBM stem/progenitor cells. (A) Neurosphere formation assay. The clonogenic capacity of control (NT) and CLIC1 silenced (sh) cells was evaluated by plating cells in methilcellulose-containing medium. After 15 days, each plate was examined under a light microscope, and the total number of neurospheres was determined. (B) CLIC1 silencing leads to impaired neurosphere formation after serial passages. No difference was observed in clonogenic capacity between CLIC1 silenced and control cells at the third re-plating when CLIC1 silenced cells re-expressed the protein (C). (D) Growth curve of control (NT) and CLIC1 silenced (sh) cells isolated from 3 GBM samples was measured by 3-(4, 5-dimethylthiazol-2-yl)-2, 5-diphenyltetrazolium bromide (MTT) assay. Three independent experiments were performed; error bars represent 95% confidence intervals; ** $p<0.001$. GLM tests of between-subjects effects showed statistically significant difference in all patients for the relative cell growth according to the time, the interference, and the interaction between those two variables. (E) Control (NT) and CLIC1 silenced (sh) neurospheres isolated from 3 patient samples were subjected to BrdU incorporation assay: BrdU-positive cells were quantified by immunofluorescence. Immunostained cells were counted at 20X magnification, five fields for each sample (average cell number per field was 150). For results in panels (A, B and E) an unpaired two-sided Student's test was used. Three independent experiments were performed; error bars represent 95% confidence intervals; ** $p < 0.001$, ** $p < 0.0001$, n. s. no significance.

Supplementary Figure 5

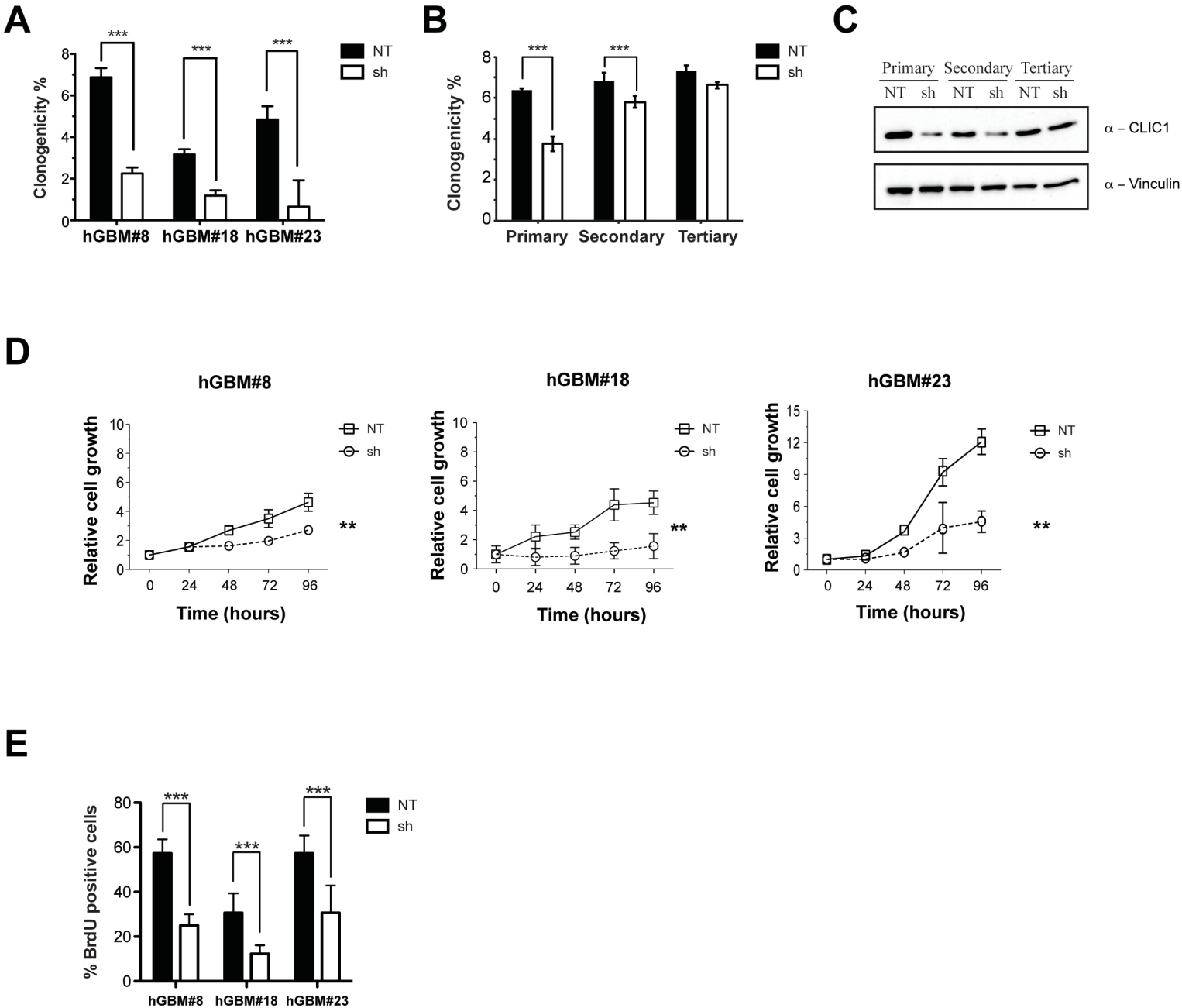

Supplementary Figure 6. Effect of CLIC1 silencing on cell cycle distribution and apoptosis of patient-derived GBM neurospheres. (A) Cells were fixed and stained with PI for the DNA content analysis by using flow cytometry (FACS). The cell cycle distribution within the total cell population is shown as histograms with the percentage of cells in the cell cycle phases indicated for NT and CLIC1 silenced (sh) cells. The results are representative of three experiments. (B and C) Apoptosis detection in CLIC1 silenced (sh) and NT cells. The percentages of apoptotic cells in the cultures were analysed by PI staining for DNA content analysis by using flow cytometry (FACS) (B) or by immunofluorescent detection of cleaved caspase 3 (C). Results shown are relative to three independent experiments; error bars represent 95% confidence intervals; p values are two-sided (Student t test).

Supplementary Figure 6

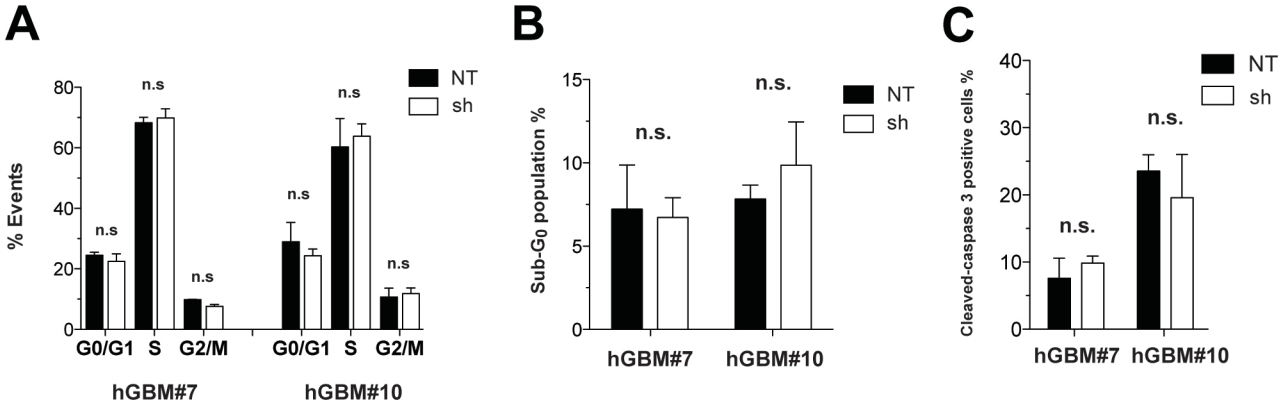

Supplementary Figure 7. Effect of CLIC1 silencing on *in vivo* tumorigenicity. (A) Kaplan-Meier survival curve of mice intracranially transplanted with 10^5 control (NT) and CLIC1 silenced (sh) hGBM#18 cells and hGBM#22 cells. Number of mice at risk expressed as weeks [number of mice at risk]: 0[4], 9.1[4], 9.3[3], 10.0[2], 10.4[1] for hGBM#18 NT; 0 [4], 10 [4], 13.1[3], 16.6[2], 16.8[1] for hGBM#18 sh group. Data are from one experiment with four mice. 0[5], 5.6[5], 8.4[4], 9[2] for hGBM#22 NT; 0[5], 10.5[5], 10.8[4], 11.8[2], 12[1] for hGBM#22 sh. Data are from one experiment with five mice. P-value was calculated with log rank test: * $p < 0.05$, ** $p < 0.001$, hGBM#18: Chi square = 4.47, d. f. 1; hGBM#22: Chi square = 9.04 , d. f. 1. (B) Representative immunohistochemical staining of controls and CLIC1 silenced xenograft tumors derived from hGBM#18 and hGBM#22 cells. H&E, CLIC1, hNuclei and GFP staining on adjacent sections are shown (scale bar= 3mm for H&E; scale bar= 300μm for IHC).

Supplementary Figure 7

A

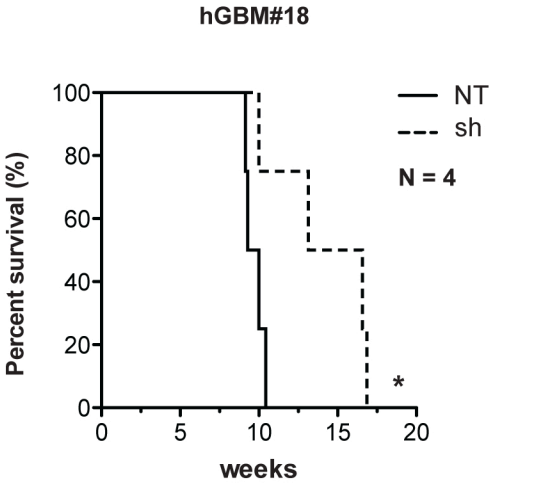

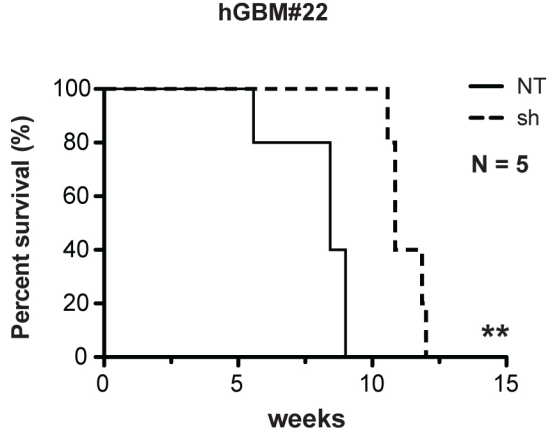

B